Available online at www.sciencedirect.com
ScienceDirect
Journal of the European Ceramic Society 31 (2011) 79–84
www.elsevier.com/locate/jeurceramsoc

Preparation of YSZ/Al_2O_3 micro-laminated coatings and their influence on the oxidation and spallation resistance of MCrAlY alloys

Junguo Gao, Yedong He *, Deren Wang

Beijing Key Laboratory for Corrosion, Erosion and Surface Technology, University of Science and Technology Beijing, 100083 Beijing, PR China

Received 7 March 2010; received in revised form 3 August 2010; accepted 7 August 2010
Available online 17 September 2010

Abstract

YSZ/Al_2O_3 micro-laminated coatings were successfully prepared on the surface of MCrAlY substrates by means of electrolytic deposition and microwave sintering. The as-prepared YSZ/Al_2O_3 coatings were characterized by high-resolution field emission SEM and XRD. Laminated structures of alternate YSZ and Al_2O_3 layers were observed in the coating with the phase composition of Y_2O_3 stabilized t-ZrO_2, α-Al_2O_3 and θ-Al_2O_3. High-temperature cyclic oxidation test at 1000 °C in air was also performed to investigate the oxidation and spallation resistance of such coatings on MCrAlY substrates. The results indicate that such coatings exhibit not only excellent oxidation resistance but also good spallation resistance under thermal cycling due to the structure of multi-sealed Al_2O_3 layers and the preferable high-temperature mechanical properties induced by the designed laminated composite structures, respectively.

Keywords: Al_2O_3; ZrO_2; Nanocomposites; Microwave processing; Oxidation and spallation resistance

1. Introduction

MCrAlY coatings (M = Ni, Co or Ni and Co) have been widely used as bond coat (BC) beneath a ceramic top coat in thermal barrier coating (TBC) systems for oxidation protection of the underlying superalloy part since 1970s.[1] It is generally accepted that the growth rate, morphology, microstructure and adherence of the aluminum-based thermally grown oxide (TGO) scale which forms on the BC surface during high-temperature service is of crucial importance for TBC life.[2] However, after long term exposure and thermal cycling, the TGO is prone to cracking and spallation due to the thermal expansion mismatch between the oxide and the metallic substrate which may finally lead to the destructive failure of the ceramic top coat.[3] In order to circumvent such a drawback, it is an effective way to add a transition layer to limit to the maximum possible extended oxygen diffusion and improve the interface state between MCrAlY and the ceramic top coat.

Layered ceramic composites have been proposed as an excellent design to enhance the strength reliability of ceramic components as well as to improve their fracture toughness by means of energy release mechanisms, such as crack deflection or crack bifurcation.[4–6] Ho and Suo[7] found that there is a critical thickness for the constrained brittle layer bonded between tougher substrates under residual and applied stresses during the investigation of tunneling cracks (such a crack initiates from an equi-axed flaw, confined by the substrates, tunneling in the brittle layer) and below the thickness, no tunneling cracks occurred regardless of the size of original cracks. So decreasing the thickness of layers is very helpful to suppress crack extension.

As an effective way to synthesize nanometer/submicrometer films or coatings, electro-deposition has the advantages of simpler process and lower cost compared to other manufacturing routes such as, for example, Chemical Vapor Deposition (CVD) or Physical Vapor Deposition (PVD) thin film processes. As early as 1993, He et al.[8,9] developed the electrochemical method to fabricate oxide coatings or films, such as Al_2O_3, ZrO_2 and Y_2O_3, etc. Yao et al.[10,11] prepared ZrO_2/Al_2O_3 micro-laminated coatings employing the same method. But the densification of the coating was not so satisfactory under conventional sintering. Compared with conventional sintering, microwave sintering is a novel technique that has gained considerable attention owing to its distinct advantages, such as fast and volumetric heating, enhancement in densification and selective heating of specific

* Corresponding author. Tel.: +86 010 62332715; fax: +86 010 62332715.
E-mail address: htgroup@mater.ustb.edu.cn (Y. He).

0955-2219/$ – see front matter © 2010 Elsevier Ltd. All rights reserved.
doi:10.1016/j.jeurceramsoc.2010.08.010

regions or phases in a mixture or composite.[12–14] In microwave sintering, electromagnetic waves interact with the ceramics, leading to volumetric heating through dielectric losses. Such a volumetric heating may result in ceramics with a more uniform and fine-grained microstructure over conventional sintering. Over years, various structural ceramics and composites such as CeO_2–ZrO_2, Y_2O_3–ZrO_2, and Al_2O_3 have been successfully synthesized by microwave sintering.[15–17]

In the present study, YSZ/Al_2O_3 micro-laminated coatings were prepared on MCrAlY substrates by electro-deposition and microwave sintering processes. The influence on the oxidation and spallation resistance of MCrAlY substrates was also investigated and mechanisms accounting for such effects are discussed.

2. Experimental procedure

Micro-laminated coatings were deposited onto surfaces of MCrAlY substrates by cathodic electrolytic deposition. 0.1 mol/L $Zr(NO_3)_4{\cdot}5H_2O$ with 8 mol% $Y(NO_3)_3{\cdot}6H_2O$ solution in absolute ethanol and 0.1 mol/L $Al(NO_3)_3{\cdot}9H_2O$ solution in absolute ethanol were used for electro-deposition. All reagents were analytically pure from Beijing Chemical Reagents Company (Beijing, China). The deposition process was conducted under constant current of 5 mA/cm^2. The electrochemical cell comprised a cathodic MCrAlY substrate (15 mm × 10 mm × 3 mm) centered between two parallel graphite counter electrodes (25 mm × 15 mm), one electrode with 15 mm form the other. The nominal composition of MCrAlY alloy is Ni–32Co–20Cr–8Al–0.5Y given by the smelting manufacturer. All surfaces of sample were ground to #1500 abrasive paper (Ra = 3.14 μm), followed by ultrasonic cleaning with ionized water and ethanol. The deposition time was 60 s for each layer and pre-heat treatment after each deposition was performed in air at 300 °C for 30 min. YSZ and Al_2O_3 layers were deposited on all the surfaces of the substrate alternately during electro-deposition. The final laminated coatings were then embedded in graphite powder and the samples were then sintered by microwave at the measured temperature of about 900 °C for 20 min. The microwave frequency was 2450 MHz and the average power of the microwave furnace was 900 W. A hydrostatic pressure of 5 MPa was applied on the graphite powder and sample during microwave sintering.

High-temperature cyclic oxidation test at 1000 °C was carried out to assess the influence of micro-laminated coatings on oxidation and thermal cyclic spallation resistance of the substrates. Quartz crucibles were used to accommodate different samples. The samples and quartz crucibles were measured in weight at the beginning using the electronic balance with an accuracy of 100 μg and were then exposed to the condition of high-temperature oxidation for a period of 10 h. After that, the samples were removed from the furnace, cooled to room temperature by natural cooling with the cooling rate of about 1 K/s and reweighed to obtain the mass gain of the oxidized samples and mass loss of the stripped samples before they were put back to the furnace again. The cyclic oxidation lasted for 200 h. The data weighed in milligram were then divided by the surface area of corresponding samples in square centimeter to plot the kinetic curves.

Si substrate was adopted to observe the cross-section morphology of YSZ/ZrO_2 micro-laminated coating due to its electrical conductivity and brittle fracture characteristic. The cross-section and surface images of the coating were characterized by high-resolution field emission SEM. Phases of the prepared coatings and oxide scales formed after oxidation were both analyzed by X-ray diffraction (CuKα, λ = 0.15406 nm, step wise of 0.02°, continuous scanning). In order to avoid the formation of cracks in the vicinity of the coatings during mounting, Ni protective coatings were deposited onto the oxidation samples by electroless plating.

3. Results

3.1. Characterization of YSZ/Al_2O_3 micro-laminated coatings

Fig. 1 shows the cross-section and surface morphologies of YSZ/Al_2O_3 micro-laminated coatings obtained by means of electro-deposition and microwave sintering. Fig. 1a presents six alternate layers of YSZ and Al_2O_3 which is consistent with deposition process and the average thickness of each layer is 100 nm, approximately. The interfaces between layers are not enough discriminated but no flaws or cracks can be obviously detected in the coating. Two main reasons may be responsible for the blurry interfaces. For one thing, the coating is prepared by wet chemical method, complicated processes such as dehydration, transforma-

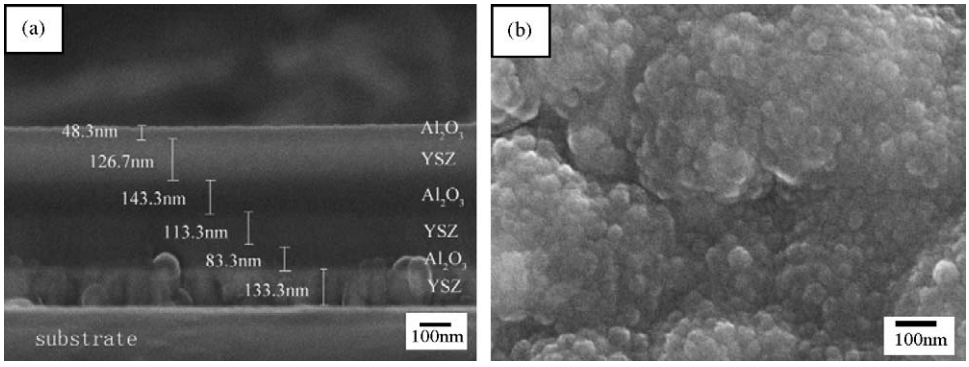

Fig. 1. FE-SEM images of YSZ/Al_2O_3 micro-laminated coatings via microwave sintering: (a) cross-section; (b) surface.

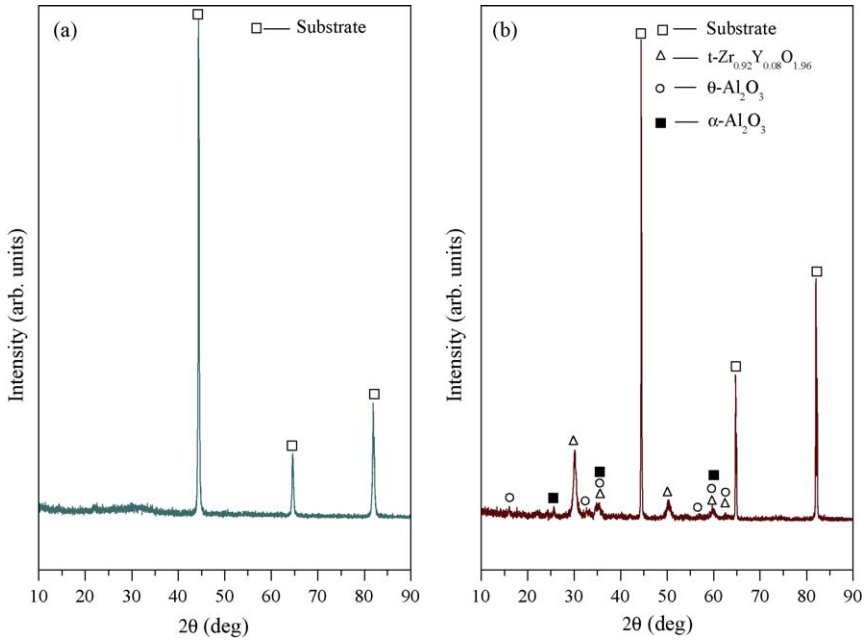

Fig. 2. XRD spectra of YSZ/Al_2O_3 micro-laminated coatings: (a) pre-heat treatment at 300 °C; (b) microwave sintering.

tion and diffusion may come up during sintering process. For the other thing, each layer of the coating is so thin that it may be close to the resolution limit of scanning electron microscopy (about 2 nm under 10 kV). Fig. 1b illustrates the surface morphology of micro-laminated coatings. Due to microwave sintering, the coating is very compact and composed of nano-particles with the size of about 40 nm. Compared with such coatings prepared through conventional sintering,[10,11] the laminated coatings sintered by microwave sintering are much denser. In particular, no micro-holes can be detected at the resolution of the picture.

Fig. 2 shows the XRD spectra of YSZ/Al_2O_3 micro-laminated coatings on stainless steel substrates after pre-heat treatment of each layer at 300 °C and subsequent microwave sintering of the laminated coating, respectively. Due to the thickness of micro-laminated coating much lower than the penetration depth of X-ray diffraction (5–10 μm on the condition) strong diffraction peaks of the substrate are identified. Besides that, there are only peaks corresponding to the substrate for coating submitted only to pre-heat treatment. It means that no crystallization process of ZrO_2 and Al_2O_3 occurred after pre-heat treatment of each layer at 300 °C during the preparation process (Fig. 2a). Then after microwave sintering under pressure for 20 min, phase transformations took place and Y_2O_3 stabilized t-ZrO_2, α-Al_2O_3 and θ-Al_2O_3 were identified in the micro-laminated coatings after crystallization (Fig. 2b).

3.2. High-temperature cyclic oxidation test of YSZ/Al_2O_3 micro-laminated coatings on MCrAlY substrates

Fig. 3 displays the results of cyclic oxidation test at 1000 °C in air for 200 h. It can be seen from Fig. 3a that all samples coated with six layers of single-phase YSZ (6Z), Al_2O_3 (6A) or YSZ/Al_2O_3 (3ZA) micro-laminated coatings greatly improved the resistance of MCrAlY substrate to high-temperature oxidation. Among the three laminate coatings, single-phase YSZ coating has relatively bad oxidation resistance owing to ZrO_2 being an oxygen ion conductor with good oxygen diffusion ability and to the formation of cracks (see Section 3.3) and single-phase Al_2O_3 coating shows a severe spallation during thermal cycling due to its thermal expansion mismatch ($8.0 \times 10^{-6}\,K^{-1}$ for Al_2O_3 and $17 \times 10^{-6}\,K^{-1}$ for Ni-based superalloy at 1000 °C) with the alloy substrate. In contrast, YSZ/Al_2O_3 micro-laminated composite coatings exhibit the optimal protection effects against oxidation and thermal cyclic spallation with less than 0.5 mg/cm^2 mass gain and 0.1 mg/cm^2 spallation mass.

3.3. Characterization of samples after high-temperature cyclic oxidation test

Surface morphologies of samples after oxidation at 1000 °C are shown in Fig. 4. The blank sample shows a relatively rough surface with needle-like and whisker morphologies which are the typical morphology of θ-Al_2O_3.[18,19] Cracks can be identified both on the single-phase YSZ coating and Al_2O_3 coating and cracking is particularly severe with regard to the Al_2O_3 coating, which is consistent with the spallation curve. Compared with single-phase YSZ and Al_2O_3 micro-laminated coatings, the surface of YSZ/Al_2O_3 composite coatings is much flatter and crack-free, as shown in Fig. 4d.

Fig. 5 shows the cross-section micrographs of samples after oxidation at 1000 °C for 200 h. Here, thermally grown oxide (TGO) of blank sample after oxidation is comparatively thicker and contains through-thickness microcracks and voids. With regard to the samples with YSZ and Al_2O_3 single-phase coatings, their TGO are thinner than the blank sample but through-thickness microcracks also develop in the TGO layer. The deposited Al_2O_3 coating is not clearly visible in Fig. 5c due

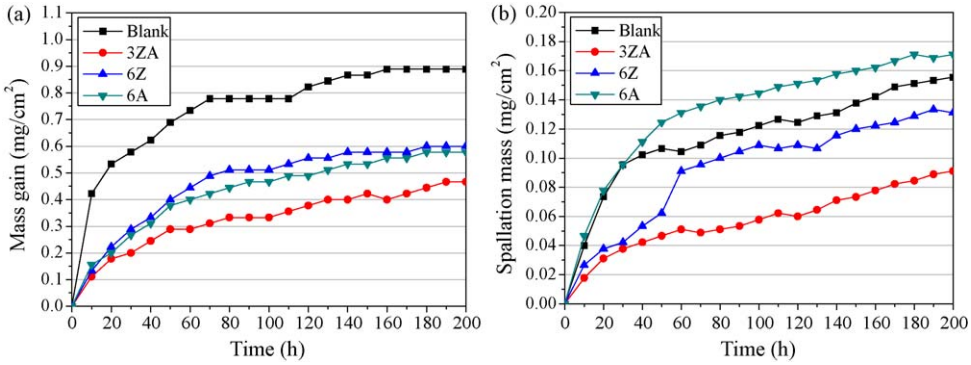

Fig. 3. Oxidation kinetic curves of samples with different micro-laminated coatings: (a) mass gain versus time; (b) spallation mass versus time (Z: 1 layer of YSZ; A: 1 layer of Al_2O_3, the same below).

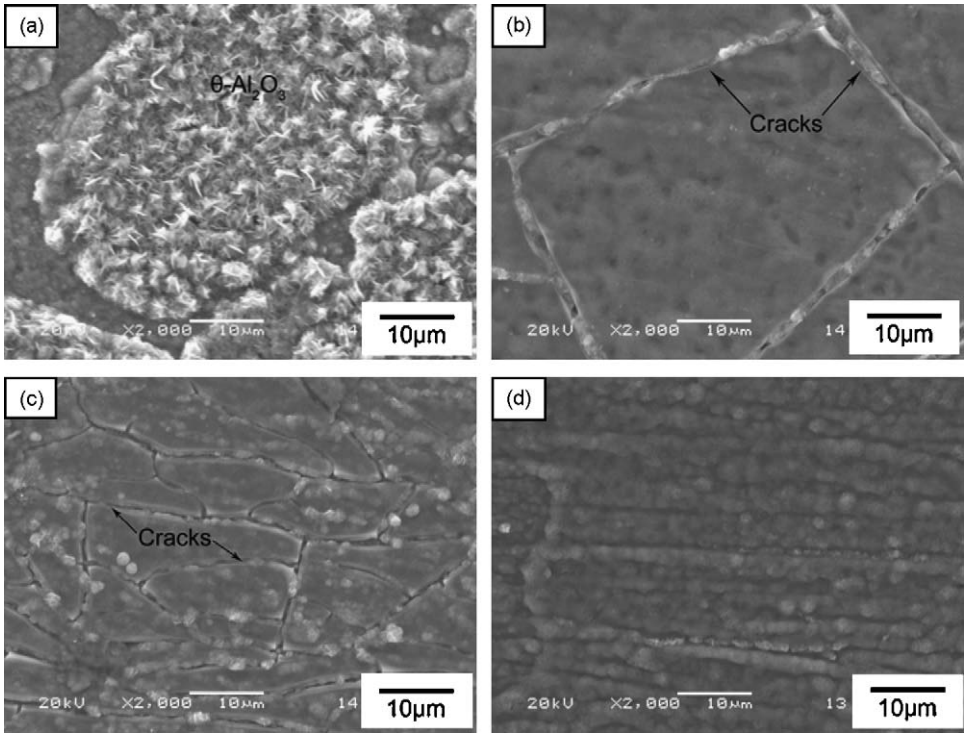

Fig. 4. Surface morphologies of samples after oxidation: (a) blank; (b) 6Z; (c) 6A; (d) 3ZA.

to its similar composition with TGO. Compared with the samples mentioned above, the sample with YSZ/Al_2O_3 composite coating has extremely thin and compact TGO layer. However, the laminated structure of composite coating is not identified as shown in Fig. 5d due to the element diffusion from the substrate to the coating and in the coating itself during high-temperature cyclic oxidation.

Fig. 6 shows the XRD analysis of samples with different micro-laminated coatings after oxidation at 1000 °C for 200 h. Strong diffraction peaks of MCrAlY alloy substrate are detected owing to the thin thickness of micro-laminated coating and TGO. All of the samples exhibit the α-Al_2O_3 phase and the blank sample also contains a certain amount of θ-Al_2O_3 which corresponds to the analysis in Fig. 4a. Besides, Y_2O_3 stabilized t-ZrO_2 is also identified in the YSZ and YSZ/Al_2O_3 micro-laminated coatings.

4. Discussion

4.1. Mechanisms for the improvement of high-temperature oxidation resistance

It is known that dense and defect-free α-Al_2O_3 layer is considered to be the most effective diffusion barrier in protecting alloy substrates from oxidation owing to its extremely low oxygen diffusion coefficient (about 1×10^{-23} m^2/s at 1300 °C).[20] As a result, it is widely used in oxide ceramic coatings. Fig. 7 shows the model of oxygen diffusion in the micro-laminated YSZ/Al_2O_3 coating. Multi-sealed Al_2O_3 layers are formed in the composite micro-laminated coatings. In spite of ZrO_2 being an oxygen ion conductor, the coating can suppress the inward diffusion of oxygen to a certain low degree and finally reduce the oxidation rate of substrate under high temperatures.

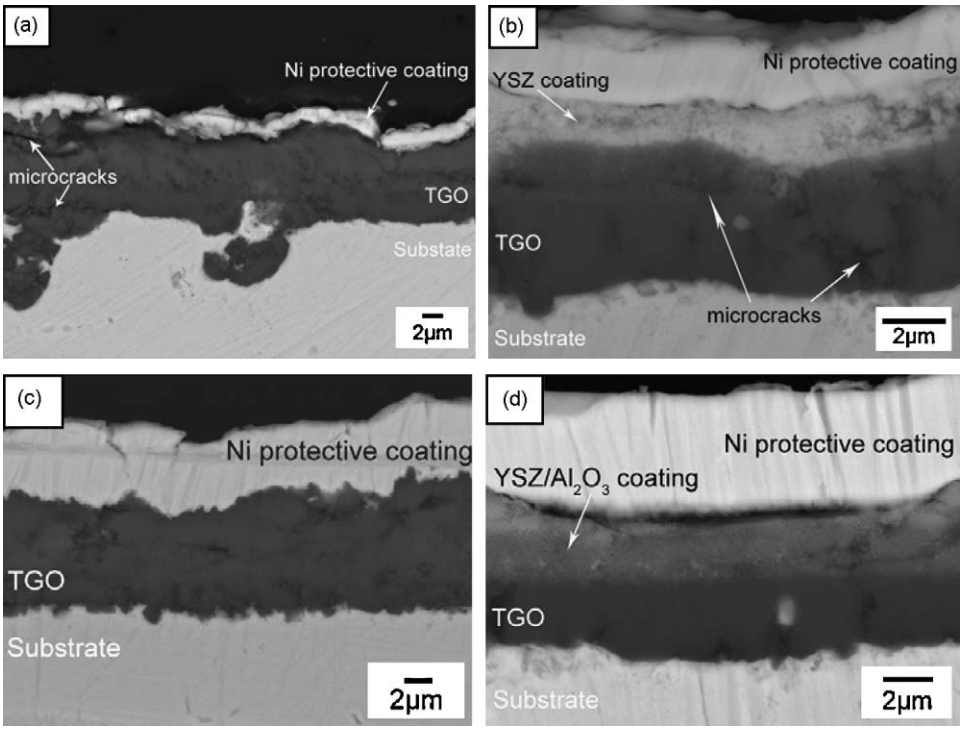

Fig. 5. FE-SEM cross-section micrographs of samples after oxidation: (a) blank; (b) 6Z; (c) 6A; (d) 3ZA.

4.2. Mechanisms for the improvement of spallation resistance under thermal cycling

It has been demonstrated that multilayered composite ceramics are an alternative choice for the design of structural ceramics with improved fracture toughness, strength and reliability. It is found that the laminated system exhibits an excellent fracture toughness which is higher than twice the value determined for the monolithic material.[21] The reason is that the laminated ceramics have good flaw tolerance and crack resistance. It can reduce the crack driving force at the crack tip by means of energy release mechanisms, such as crack deflection or crack bifurcation.[22] With regard to the current laminated system, since ZrO_2 exhibits a coefficient of thermal expansion ($11–13 \times 10^{-6}\,K^{-1}$) close to the one of the metals ($14–17 \times 10^{-6}\,K^{-1}$) and better fracture toughness than Al_2O_3, the YSZ/Al_2O_3 laminated composite structure can relax thermal stress generated during high-temperature cycles.

As mentioned in literature,[23] thermal stresses generated during cooling due to the difference in coefficients of thermal expansion between the substrate (metal) and the layer (oxide)

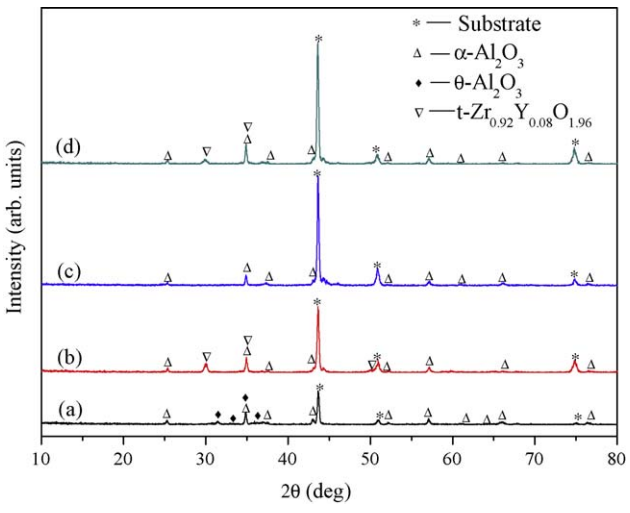

Fig. 6. XRD spectra of oxidation samples with different micro-laminated coatings: (a) blank; (b) 6Z; (c) 6A; (d) 3ZA.

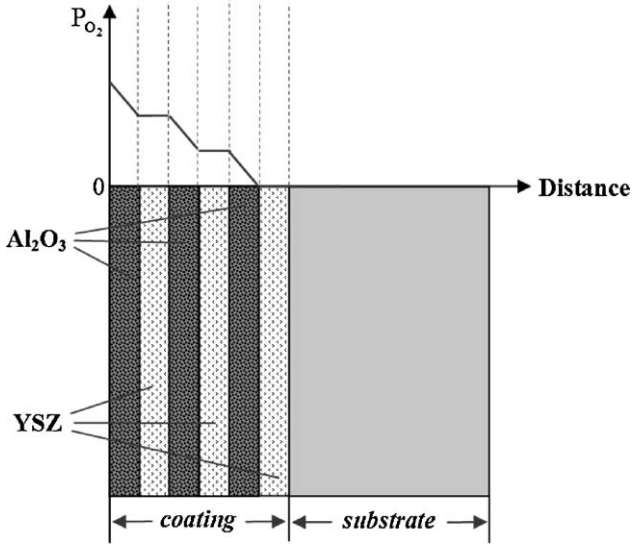

Fig. 7. Model of oxygen diffusion in YSZ/Al_2O_3 micro-laminated coatings.

can be expressed as follows:

$$\sigma_{Ox} = \frac{-E_{Ox}(\alpha_{Ox} - \alpha_M)\ \Delta T}{(1-\nu)(1+2\,t_{Ox}E_{Ox}/t_M E_M)}, \quad (1.1)$$

where α_M and α_{Ox} are the (assumed constant) linear coefficients of thermal expansion for metal and oxide, respectively, E_M and E_{Ox} are the apparent Young modulus for metal and oxide, respectively, and t_M and t_{Ox} are the thicknesses for metal and oxide, respectively. ΔT is the temperature difference across cooling and ν is the Poisson ratio. In cases where the oxide is very thin relatively to the thickness of the metal, the last term in the denominator of Eq. (1.1) can be neglected, yielding to:

$$\sigma_{Ox} = \frac{-E_{Ox}(\alpha_{Ox} - \alpha_M)\ \Delta T}{1-\nu}. \quad (1.2)$$

Note that in the laminated YSZ/Al_2O_3 composite coating, $E_{composite}$ is less than $E_{Al_2O_3}$ and $\alpha_{composite}$ is larger than $\alpha_{Al_2O_3}$. As mentioned above, thermal expansion coefficients of Al_2O_3 and YSZ are lower than that of metal, so the thermal stresses generated in the YSZ/Al_2O_3 composite coating are relatively lower than that in single-phase Al_2O_3 coating.

Therefore, the improved fracture toughness and lower thermal stresses generated during cooling induced by the design of YSZ/Al_2O_3 micro-laminated composite coating result in the improved high-temperature mechanical properties and thus improved spallation resistance of MCrAlY alloy under thermal cycling significantly.

5. Conclusions

In this contribution, oxidation and spallation resistance of micro-laminated YSZ/Al_2O_3 composite coatings on MCrAlY alloys under thermal cyclic oxidation were investigated and following conclusions can be drawn:

(1) Dense micro-laminated YSZ/Al_2O_3 coatings were successfully fabricated by means of electro-deposition and microwave sintering processes.
(2) Compared with single-phase YSZ or Al_2O_3 coatings, YSZ/Al_2O_3 micro-laminated coatings are more conductive to the resistance of MCrAlY substrate to high-temperature oxidation and spallation.
(3) Such protection effects result from the formation of multi-sealed Al_2O_3 layers in the coating and the preferable high-temperature mechanical properties induced by the design of micro-laminated composite structures.

Acknowledgement

This work is financially supported by Chinese National Natural Science Foundation (Grant. 50771021).

References

1. Bose S, DeMasi-Marcin J. Thermal barrier coating experience in gas turbine engines at Pratt & Whitney. *J Thermal Spray Technol* 1997;**6**:99–104.
2. Busso EP, Lin J, Sukurai S, Nakayama M. A mechanistic study of oxidation-induced degradation in a plasma-sprayed thermal barrier coating system. Part I: Model formulation. *Acta Mater* 2001;**49**: 1515–28.
3. Gil A, Naumenko D, Vassen R, Toscano J, Subanovic M, Singheiser L, Quadakkers WJ. Y-rich oxide distribution in plasma sprayed MCrAlY-coatings studied by SEM with a cathodoluminescence detector and Raman spectroscopy. *Surf Coat Technol* 2009;**204**:531–8.
4. He MY, Hutchinson JW. Crack deflection at an interface between dissimilar elastic materials. *Int J Solids Struct* 1989;**25**:1053–67.
5. Oechsner M, Hillman C, Lange FF. Crack bifurcation in laminar ceramic composites. *J Am Ceram Soc* 1996;**79**:1834–8.
6. Sánchez-Herencia AJ, James L, Lange FF. Bifurcation in alumina plates produced by a phase transformation in central, alumina/zirconia thin layers. *J Eur Cer Soc* 2000;**20**:1297–300.
7. Ho S, Suo Z. Tunneling cracks in constrained layers. *J Appl Mech-T ASME* 1993;**60**:890–4.
8. Lu XY, Zhu RZ, He YD. Electrodeposited thin oxide films. *Surf Coat Technol* 1996;**79**:19–24.
9. Lu XY, Zhu RZ, He YD. Electrophoretic deposition of MCrAlY overlay-type coatings. *Oxid Met* 1995;**43**:353–62.
10. Yao MM, He YD, Wang DR, Gao W. The oxidation resistance of Fe-^{13}Cr alloy with micro-laminated (ZrO_2–Y_2O_3)/(Al_2O_3–Y_2O_3) films. *J Rare Earth* 2005;**23**:559–63.
11. Yao MM, He YD, Gou YJ, Gao W. Preparation of ZrO_2–Al_2O_3 micro-laminated coatings on stainless steel and their high temperature oxidation resistance. *Trans Nonferrous Met Soc China* 2005;**15**: 1388–93.
12. Wang J, Binner J, Pang Y, Vaidhyanathan B. Microwave-enhanced densification of sol–gel alumina films. *Thin Sol Films* 2008;**516**: 5996–6001.
13. Huanga SG, Li L, Van der Biest O, Vleugels J. Microwave sintering of CeO_2 and Y_2O_3 co-stabilised ZrO_2 from stabiliser-coated nanopowders. *J Eur Ceram Soc* 2007;**27**:689–93.
14. Mazaheri M, Zahedi AM, Hejazi MM. Processing of nanocrystalline 8 mol% yttria-stabilized zirconia by conventional, microwave-assisted and two-step sintering. *Mater Sci Eng A* 2008;**492**:261–7.
15. Travitzky NA, Goldstein A, Avsian O, Singurindi A. Microwave sintering and mechanical properties of Y-TZP/20 wt.% Al_2O_3 composites. *Mater Sci Eng A* 2000;**286**:225–9.
16. Goldstein A, Travitzky N, Singurindy A, Kravchik M. Direct microwave sintering of yttria-stabilized zirconia at 2.45 GHz. *J Eur Ceram Soc* 1999;**19**:2067–72.
17. Xie Z, Wang C, Fan X, Huang Y. Microwave processing and properties of Ce–Y-ZrO_2 ceramics with 2.45 GHz irradiation. *Mater Lett* 1999;**38**:190–6.
18. Strauss D, Müller G, Schumacher G, Engelko V, Stamm W, Clemens D, Quaddakers WJ. Oxide scale growth on MCrAlY bond coatings after pulsed electron beam treatment and deposition of EBPVD-TBC. *Surf Coat Technol* 2001;**135**:196–201.
19. Iwamoto H, Sumikawa T, Nishida K, Asano T, Nishida M, Araki T. High temperature oxidation behavior of laser clad NiCrAlY layer. *Mater Sci Eng A* 1998;**241**:251–8.
20. Heuer AH. Oxygen and aluminum diffusion in α-Al_2O_3: How much do we really understand? *J Eur Ceram Soc* 2008;**28**:1495–507.
21. Bermejo R, Torres Y, Baudín C, Sánchez-Herencia AJ, Pascual J, Anglada M, Llanes L. Threshold strength evaluation on an Al_2O_3–ZrO_2 multilayered system. *J Eur Ceram Soc* 2007;**27**:1443–8.
22. Bermejo R, Pascual J, Lube T, Danzer R. Optimal strength and toughness of Al_2O_3–ZrO_2 laminates designed with external or internal compressive layers. *J Eur Ceram Soc* 2008;**28**:1575–83.
23. Birks N, Meier GH, Pettit FS. *Introduction to the High-temperature Oxidation of Metals*. New York, NY, USA: Cambridge University Press; 2006. pp. 138–139.